JGR Biogeosciences

RESEARCH ARTICLE
10.1029/2023JG007852

Grass Evolutionary Lineages Can Be Identified Using Hyperspectral Leaf Reflectance

Ryan Slapikas[1], Stephanie Pau[1], Ryan C. Donnelly[2], Che-Ling Ho[3], Jesse B. Nippert[2], Brent R. Helliker[3], William J. Riley[4], Christopher J. Still[5], and Daniel M. Griffith[5,6]

[1]Department of Geography, Florida State University, Tallahassee, FL, USA, [2]Division of Biology, Kansas State University, Manhattan, KS, USA, [3]Department of Biology, University of Pennsylvania, Philadelphia, PA, USA, [4]Climate and Ecosystem Sciences Division, Lawrence Berkeley National Lab, Berkeley, CA, USA, [5]Department of Forest Ecosystems & Society, Oregon State University, Corvallis, OR, USA, [6]Department of Earth & Environmental Sciences, Wesleyan University, Middletown, CT, USA

Key Points:

- Globally dominant grass lineages are identifiable using hyperspectral leaf signatures
- Key wavelengths for separating grass lineages were visible, red-edge and shortwave infrared regions, rarely measured by multispectral sensors
- Hyperspectral sensors have the potential to improve remote sensing identification of grass functional types over multispectral sensors

Supporting Information:

Supporting Information may be found in the online version of this article.

Correspondence to:

R. Slapikas and S. Pau,
res09e@fsu.edu;
spau@fsu.edu

Citation:

Slapikas, R., Pau, S., Donnelly, R. C., Ho, C.-L., Nippert, J. B., Helliker, B. R., et al. (2024). Grass evolutionary lineages can be identified using hyperspectral leaf reflectance. *Journal of Geophysical Research: Biogeosciences*, *129*, e2023JG007852. https://doi.org/10.1029/2023JG007852

Received 16 OCT 2023
Accepted 2 JAN 2024

Abstract Hyperspectral remote sensing has the potential to map numerous attributes of the Earth's surface, including spatial patterns of biological diversity. Grasslands are one of the largest biomes on Earth. Accurate mapping of grassland biodiversity relies on spectral discrimination of endmembers of species or plant functional types. We focused on spectral separation of grass lineages that dominate global grassy biomes: Andropogoneae (C_4), Chloridoideae (C_4), and Pooideae (C_3). We examined leaf reflectance spectra (350–2,500 nm) from 43 grass species representing these grass lineages from four representative grassland sites in the Great Plains region of North America. We assessed the utility of leaf reflectance data for classification of grass species into three major lineages and by collection site. Classifications had very high accuracy (94%) that were robust to site differences in species and environment. We also show an information loss using multispectral sensors, that is, classification accuracy of grass lineages using spectral bands provided by current multispectral satellites is much lower (accuracy of 85.2% and 61.3% using Sentinel 2 and Landsat 8 bands, respectively). Our results suggest that hyperspectral data have an exciting potential for mapping grass functional types as informed by phylogeny. Leaf-level hyperspectral separability of grass lineages is consistent with the potential increase in biodiversity and functional information content from the next generation of satellite-based spectrometers.

Plain Language Summary Understanding and identifying changes in plant diversity along broad environmental gradients requires scalable and reliable data. Spectroscopy has been shown to provide data across scales with the ability to measure plant reflectance at various extents (e.g., leaf, plot, and landscapes) with high spectral resolution and broad coverage of the electromagnetic spectrum (350–2,500 nm). In grasses, evolutionary lineage captures major axes in plant biodiversity and functional variation. We show that identifying grass evolutionary lineages from spectroscopy is possible based on common characteristics in their leaf-level spectra. We classified 43 grass species from four sites in North America into their respective evolutionary lineages with very high accuracy (>90%) based on similarities in their leaf spectra. Classifying grass species into lineages using coarser spectral resolution data, similar to existing multispectral satellites, Sentinel 2 and Landsat 8, resulted in lower accuracy due to a loss of information from decreasing the spectral resolution. Grass lineages likely have similar spectra because of common leaf traits that evolved under similar ecological contexts. The importance of these distinctions found in the spectral reflectance of dominant grass lineages, should help our efforts in mapping and understanding grassland ecosystem function and patterns of biodiversity.

1. Introduction

A major goal for imaging spectroscopy is to remotely monitor dimensions of biodiversity (Cawse-Nicholson et al., 2021; Griffith et al., 2023a, 2023b; Rocchini et al., 2022). To that end, numerous studies have sought to relate spectral diversity to taxonomic, functional, and phylogenetic diversity across scales (e.g., Cavender-Bares et al., 2017; Schweiger et al., 2018). Leaf spectra may represent a scalable feature of field to remote sensing observations (Cavender-Bares et al., 2017, 2022; Serbin et al., 2014). The first step in using leaf spectra to scale to larger extent remote sensing observations is to identify which properties of vegetation are detectable by spectra.

Remote sensing enables continuous mapping of species distributions, functional types, and traits along environmental gradients, thereby improving understanding of linkages among plants, traits, and their ecological

contexts, as well as spatial patterns from local to global scales. Precursor sensors on the International Space Station (ISS), such as DLR Earth Sensing Imaging Spectrometer (DESIS), Hyperspectral Imager Suite (HISUI), and Earth Surface Mineral Dust Source Investigation (EMIT), and the upcoming satellite hyperspectral missions Environmental Mapping and Analysis Program (EnMAP), Copernicus Hyperspectral Imaging Mission for the Environment (CHIME), and surface biology and geology (SBG), as well as airborne missions such as NEON AOP and the AVIRIS campaigns provide repeat measurements of hundreds of narrow wavelength reflectance bands across broad spectral regions (300–2,500 nm) at ∼30 m or higher spatial resolution. The broad spectra measured can be grouped into three main regions–the visible (VIS), near-infrared (NIR), and short-wave infrared (SWIR)–each capturing different features of leaves and canopies (Ustin et al., 2004). Reflectance in the VIS region is generally dominated by pigments such as chlorophyll and carotenoids, which can indicate photosynthetic capacity (Curran et al., 1990; Gitelson & Merzlyak, 1998; Ustin et al., 2004). The NIR region is controlled by the internal structure of leaves, such as intercellular spaces within a leaf, and air-water interfaces (Jensen, 2007; Ustin et al., 2004). Lastly, the SWIR region is sensitive to differences in water content and biochemical constituents such as lignin, cellulose, and components critical for biochemistry such as leaf Nitrogen (Jensen, 2007; Ustin et al., 2004). Thus, the broad coverage of hyperspectral imaging can help discriminate between different species and traits in ways that multispectral sensors often cannot.

Related plant species can share spectral features because of similar leaf traits and niche space (Crisp et al., 2009; Meireles et al., 2020). Because traits underlie most differences in leaf spectra, and these traits have evolutionary histories and constraints, leaf spectra should contain a phylogenetic signal, a phenomenon also known as phylogenetic conservatism (Cavender-Bares et al., 2016, 2017, 2022; Schweiger et al., 2018). Early work revealing a phylogenetic signal in remote sensing observations showed that phylogeny helped explain the foliar chemistry and spectroscopic signatures among tree canopies of a lowland tropical forest (Asner & Martin, 2011). Analysis of over 540 plant species found phylogenetically driven variation in leaf reflectance, and that the spectral region with the strongest phylogenetic signals varied with lineage (Meireles et al., 2020). For example, in monocots, the visible and NIR regions were most closely associated with phylogenetic signal whereas in gymnosperms the SWIR region was most strongly associated with phylogenetic signal (Meireles et al., 2020). Spectral diversity or spectral dissimilarity from experimental plots also increases with evolutionary divergence time and was linked to variation in productivity (Schweiger et al., 2018). Phylogeny-based approaches have enabled the partitioning of sources of spectral variability in regional floras (Griffith, Byrd, Anderegg, et al., 2023) and the mapping of dominant plant lineages (Griffith et al., 2023a, 2023b). Most studies showing phylogenetic conservatism in leaf spectra, however, are limited to single sites and few sampling periods despite recognition that leaf traits are highly plastic within a given species and change under varying resource limitations (Bachle & Nippert, 2022). Thus, a key question is which leaf spectra wavelengths vary with phylogeny, and are changes in these wavelengths discernible under different environmental contexts?

The Poaceae (grasses) have radiated into one of the most diverse plant families on Earth, with over 11,500 extant species (Soreng et al., 2017). Grass-dominated ecosystems represent a model system for the early development of lineage-based classification and mapping (Griffith et al., 2020). Grasses exhibit a high degree of variation in their ecological behavior (Liu et al., 2012; Taylor et al., 2010). This variability has traditionally been grouped into coarse plant types based on photosynthetic pathway, that is, C_3 versus C_4. The distribution of C_3 and C_4 grasses is well studied, with C_4 grasses generally more abundant and more productive in warm and high light environments (Still et al., 2003). However, the C_4 photosynthetic pathway has evolved independently in at least 24 grass lineages (Aliscioni et al., 2012; Griffith et al., 2020) that differ in their ecology, climate niches, and lineage ages (Edwards & Smith, 2010; Edwards & Still, 2008). The Andropogoneae and Chloridoideae lineages are globally dominant C_4 lineages, and Pooideae is the most dominant C_3 lineage (Griffith et al., 2020; Lehmann et al., 2019). These lineages sort along environmental gradients and exhibit a very different biogeographic distribution than classic C_3–C_4 turnover would suggest (Griffith et al., 2020). Because each lineage evolved in a different ecological context, similarities among their morphological, biochemical, and physiological traits should be more accurately captured by lineage than by functional groupings based on photosynthetic pathway (Donnelly et al., 2023; Griffith et al., 2020).

Despite being one of the most species-rich Angiosperm families and dominating one of the largest biomes on Earth, the distribution of grasses remain misrepresented in ecosystem models (Still et al., 2019). This issue is significant because grassland ecosystems are threatened globally, and account for a large proportion of terrestrial productivity and are a center of biodiversity (Bond et al., 2005; Bond & Midgley, 2000; Griffith et al., 2017;

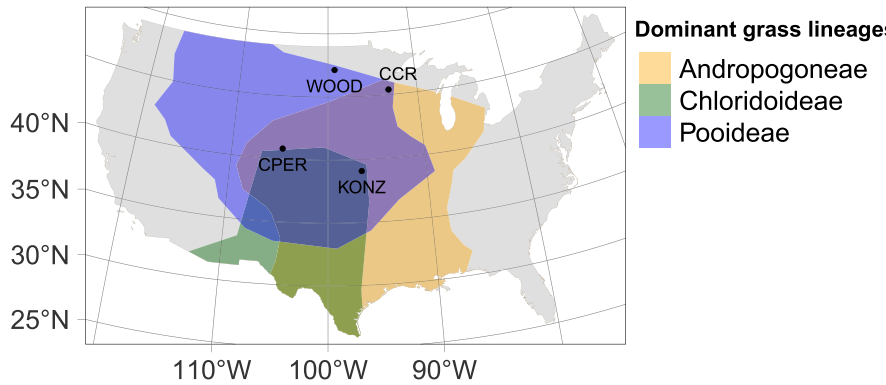

Figure 1. Map of study sites where grass species and spectra were collected. These sites are dominated by different grass lineages and span a broad environmental gradient: Colorado Plains Experimental Range (CPER; mean annual temperature (MAT) = 8.6°C, mean annual precipitation (MAP) = 344.2 mm), Konza Prairie (KONZ; MAT = 12.4°C, MAP = 870 mm), Cedar Creek Ecosystem Science Reserve (CCR; MAT = 6.7°C, MAP = 660.4 mm), and Chase Lake National Wildlife Refuge (WOOD; MAT = 4.9°C, MAP = 495 mm). Here we represented the distribution of the three major lineages by overlaying the ranges of dominant species in each lineage using the Global Biodiversity Information Facility (GBIF) web portal (http://www.gbif.org/; accessed August 2020).

Strömberg & Staver, 2022). Given the vast areas on Earth where grasses exist, their functional diversity is key to understanding global patterns of plant diversity and primary productivity. In this paper, we used spectroscopy to examine if three dominant grass lineages (Andropogoneae, Chloridoideae, and Pooideae) can be distinguished from each other based on leaf-level reflectance data from taxa in each lineage. We developed a library of grass leaf spectra from four grassland sites that span diverse grass-dominated ecoregions of North America (Figure 1). We used a classification method to investigate how well lineages group based on their spectral reflectance. We then identified which spectral regions contributed the most to separating grass lineages. Finally, we aggregated hyperspectral leaf-level spectra to the spectral resolution matching multispectral sensors and compare their classification accuracy. Our goal in this last analysis was not to perform an upscaling of our leaf reflectance data but rather to examine the information content of hyperspectral data for classifying grass lineages.

2. Methods

We analyzed leaf-level spectra from 43 grass species from four sites in North America during the summers of 2020–2022. Three of the four sites are part of the National Ecological Observatory Network (NEON): (a) Konza Prairie (KONZ), Manhattan, Kansas, (b) Colorado Plains Experimental Range (CPER), Colorado, (c) Chase Lake National Wildlife Refuge (WOOD), North Dakota, as well as (d) the Cedar Creek Ecosystem Science Reserve (CCR), Minnesota. All sites were sampled during peak greenness to account for any potential differences in phenology. Peak greenness was determined from a National Ecological Observatory Network (NEON) model using more than 15 years of Moderate Resolution Imaging Spectroradiometer (MODIS) Normalized Difference Vegetation Index (NDVI) data. These sites span a broad geographic gradient ranging from warm and dry conditions (CPER) to warm and wet (KONZ) or wet and cold (CCR) environments, and the range of photosynthetic pathway abundance varied accordingly. We grouped dominant grass species at each site into three groups (Figure 2; Table 1): Andropogoneae (n = 8 spp), Chloridoideae (n = 13 spp), and Pooideae (n = 22 spp). In total we sampled 54 species (Table S1). Notably, the small sample size of certain groups within the Panicoideae subfamily may limit broader inference. While results using all Panicoideae species did not substantively change results (Table S2), we focused on species in the Andropogoneae tribe, which is the dominant lineage within the Panicoideae subfamily and represents an independent origin of C_4 photosynthesis. Eleven species occurred in more than one site: *Andropogon gerardii*, *Bouteloua curtipendula*, *Bouteloua dactyloides*, *Bouteloua gracilis*, *Bromus inermis*, *Elymus smithii*, *Hesperostipa spartea*, *Phalaris arundinacea*, *Poa pratensis*, *Schizachyrium scoparium*, and *Sorghastrum nutans*.

Five to eight samples of fresh leaf spectra for each species were measured using an ASD FieldSpec 4 Hi-Res NG spectroradiometer with a leaf contact probe containing an internal calibrated light source and a leaf clip with the standard black surface behind the leaves (Malvern Panalytical Ltd., Malvern, United Kingdom). In the case of a

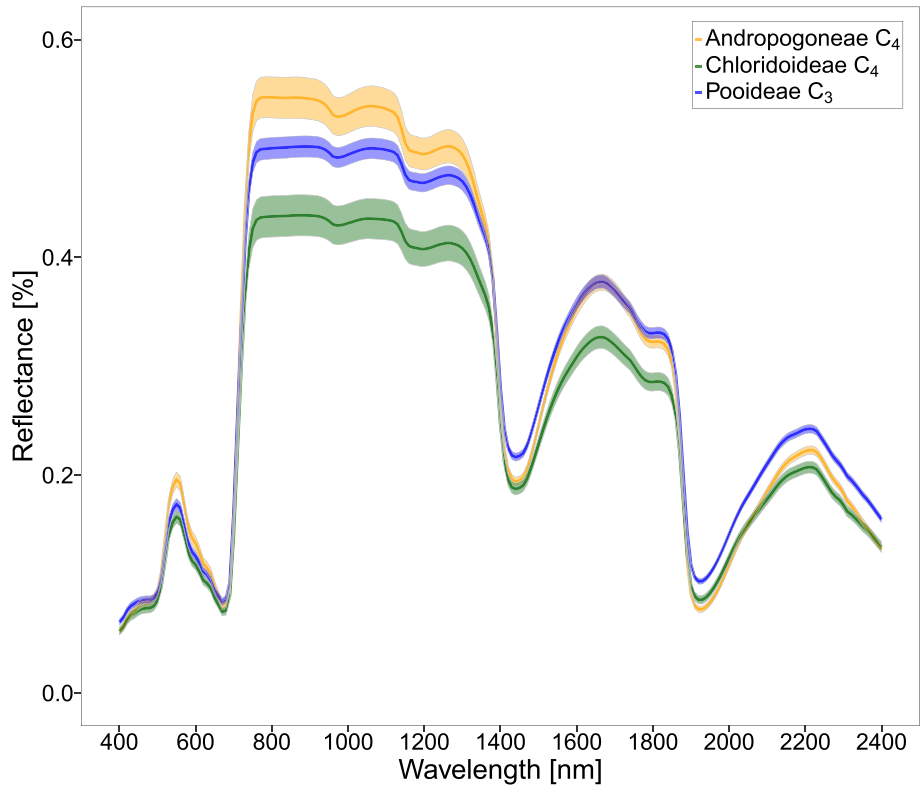

Figure 2. Mean spectra and 95% confidence interval for each of the three dominant grass lineages in the Continental United States: Andropogoneae (yellow), Chloridoideae (green), and Pooideae (blue).

single leaf area being too small to cover the area of the black background, several leaves were placed side-by-side with the adaxial surfaces oriented toward the sensor. (See Figure S1 for photographs of our measurement set-up.) Leaves were carefully placed side-by-side as close as possible to ensure no visible gaps between leaves while avoiding overlap. Occasionally, when leaves were especially narrow, small gaps were unavoidable. The FieldSpec 4 Hi-Res NG measures reflectance in the electromagnetic spectrum from 350 to 2,500 nm with 2,150 bands at 1 nm intervals. Fresh leaf spectra were measured within a 2-hr window of sampling from the field. A standard white reference built into the leaf clip (ASD Leaf Clip Version 2) was measured for calibration before each species was measured and also every 10 minutes (Hellmann et al., 2015). The spectroradiometer was set to 25 internal repetitions, allowing the spectroradiometer to reduce measurement variability and noise by measuring each leaf 25 times and then averaging the measurements to generate one spectral reflectance for the sample. The data were corrected for spectral discontinuities between the three spectroradiometer sensors using a jump correction as in (Bachmann & Heldens, 2006).

Table 1
Relative Abundance (%) of Each Lineage and the Number of Species (n) *in Each Lineage Collected at Each Site*

Site	Andropogoneae	Chloridoideae	Pooideae	Total number of unique species for each site
CCR	59% ($n = 3$)	<1% ($n = 0$)	37% ($n = 11$)	$n = 11$
CPER	0% ($n = 0$)	51% ($n = 8$)	46% ($n = 10$)	$n = 10$
KONZ	71% ($n = 8$)	19% ($n = 11$)	2% ($n = 32$)	$n = 32$
WOOD	3% ($n = 1$)	5% ($n = 4$)	90% ($n = 6$)	$n = 6$
Total number of unique species for each lineage	$n = 8$	$n = 13$	$n = 22$	$n = 43$

Note. Relative abundance was calculated by summing % cover for species at each site using data from 1 m^2 plots provided by NEON for CPER, KONZ, and WOOD, while CCR data came from NutNet (Carroll et al., 2022). Each species was represented by 5–8 leaves taken from different populations across each site (445 total observations), with 11 species occurring at multiple sites.

Spectral resampling was performed to reduce multicollinearity among predictor variables. Wavelengths shorter than 400 nm or longer than 2,400 nm were removed to address spectrally noisy regions. Then a spline interpolation with a moving window of 10 nm (Meireles et al., 2020) using the "hsdar" package (Lehnert et al., 2019) in the software R (R Core Team, 2022) was used to reduce spectral bands from 2,150 to 2,201 bands (Figure 2). Linear Discriminant Analysis (Lehmann et al., 2019) was used to classify grass lineage membership based on spectral differences among groups. LDA reduces the dimensionality of the data by maximizing the component axis across feature space. An LDA approach maximizes variation and separability between the classes. Due to the presence of correlations among numerous bands in hyperspectral data, we opted to employ LDA as a dimension reduction technique and a classifier (Garcia-Allende et al., 2008; Seetohul et al., 2013). The LDA analysis was performed using the 'caret' package (Kuhn, 2008) in the software R (R Core Team, 2022).

We first classified leaf spectra of the three dominant lineages (Andropogoneae, Chloridoideae, Pooideae) using LDA, and then classified lineages across sites. Although some lineages were not well represented at all sites ($\leq$2 species samples at some sites), limiting our classification groups to greater species representation did not substantively change results (Table S3). We used a 10-fold cross-validation with 80% of the data for training the model, and 20% to test the model's performance, rounding to the nearest integer. This cross-validation used stratified random sub-sampled data from each lineage for training and validation, but never used the same data subset twice. The overall prediction accuracy and Kappa scores were averaged. Classification accuracy is represented with confusion matrices showing their classification accuracy, sensitivity, specificity, and Kappa scores.

We used the coefficients of the linear discriminants to identify variable importance (i.e., influential bands) for separating each lineage. The linear discriminants coefficients are weights to assess the separability among groups from the input variables. We extracted k-number of linear discriminants that explained >80% of the variance in the data to assess which bands were most influential on spectra. We did this twice, once using raw spectra, which included differences in albedo (i.e., absolute differences in reflectance), and again on normalized spectra to compare individual absorption features (i.e., the shape of the spectra irrespective of differences in reflectance). Spectra were normalized using continuum removal (CR), a common method used to identify and compare absorption features across the spectra (Clark & Roush, 1984; Mutanga & Skidmore, 2004). We performed the continuum removal transformation using the "hsdar" function. Reflectance is normalized to a continuum line, which is established by connecting the local maxima of the reflectance spectrum.

To assess the classification accuracy of lineages using spectral bands provided by multispectral sensors, we implemented spectral resampling from the "hsdar" package. This links the characteristics of satellite sensors to the input spectra, generating an aggregated multispectral leaf-level spectra. The function encompasses each band's central wavelength and full-width-half-maximum values of each sensor.

3. Results

3.1. Classification Accuracy of Grass Lineages

The leaf-level spectra of three dominant grass subfamilies separated well using both the raw spectra and the normalized spectra. The overall prediction accuracy using raw spectra was 94% and the Kappa coefficient was 0.91 (Table 2a). The overall prediction accuracy and Kappa coefficient using normalized spectra were the same (Table S4a). Only two components were required to explain 100% of the variation in the spectra. The first discriminant (LD1) explained 80.8% of the variance in the raw spectra, the second discriminant (LD2) explained 19.2% of the remaining variance (Figure 3). Using the normalized spectra, LD1 explained 77.1% of the variance in the spectra and LD2 explained 22.9% of the remaining variance. While the three lineages clearly separated along LD1, Andropogoneae and Pooideae overlapped along LD2, but LD2 did separate the C_4 lineages Andropogoneae and Chloridoideae (Figure 3).

When lineages were considered by site, classification accuracy of raw spectra was 98% and the Kappa coefficient was 0.97 (Table 2b). The overall accuracy of the normalized spectra improved to 98% and the Kappa coefficient increased to 0.97 (Table S4b). Eleven components were required to explain 100% of the variation in the spectra, with the first five discriminant axes explaining over 80% of the variance in the spectra (Figure 4). Using the raw spectra the first component (LD1) explains 39% of the variation in the spectra where the second component (LD2) explains 18.4%. The third component (LD3) explained 13.1%, while the fourth and fifth components (LD4 and LD5) explained 9.5% and 8.1%, respectively.

Table 2
Classification Matrices of Leaf Spectra From LDA Models for Identifying (a) Lineages and (b) Lineages at Each Site

a.)

	Reference				
Prediction	Andropogoneae	Chloridoideae	Pooideae	Total	Prediction accuracy (%)
Andropogoneae	20	1	0	21	95%
Chloridoideae	2	20	1	23	87%
Pooideae	0	1	43	44	98%
Total	22	22	44	88	
Reference accuracy (%)	91%	91%	98%		
Overall classification accuracy = 94% and the Kappa statistic = 0.91					

b.)

	Reference											
	Andropogoneae			Chloridoideae			Pooideae					Prediction accuracy
Prediction	CCR	KONZ	WOOD	CPER	KONZ	WOOD	CCR	CPER	KONZ	WOOD	Total	(%)
Andropogoneae (CCR)	5	0	0	0	0	0	0	0	0	0	5	100%
Andropogoneae (KONZ)	0	13	0	0	0	0	0	0	0	0	13	100%
Andropogoneae (WOOD)	0	0	2	0	0	0	0	0	0	0	2	100%
Chloridoideae (CPER)	0	0	0	1	0	0	0	1	0	0	2	50%
Chloridoideae (KONZ)	0	0	0	0	18	0	0	0	0	0	18	100%
Chloridoideae (WOOD)	0	0	0	0	0	2	0	0	0	0	2	100%
Pooideae (CCR)	0	0	0	0	0	0	12	0	0	0	12	100%
Pooideae (CPER)	0	0	0	0	0	0	0	11	0	0	11	100%
Pooideae (KONZ)	0	0	0	0	0	0	0	0	15	0	15	100%
Pooideae (WOOD)	0	0	0	0	0	1	0	0	0	4	5	80%
Total	5	13	2	1	18	3	12	12	15	4	85	
Reference accuracy (%)	100%	100%	100%	100%	100%	67%	100%	91.70%	100%	100%		
Overall classification accuracy = 98% and the Kappa statistic = 0.97												

Note. Correctly identified lineages are shown on the diagonal while false positives and false negatives are shown on the off diagonals.

3.2. Identification of Spectral Band Importance

For the classification of spectra by lineage only, coefficients for the two LD axes showed that the "red edge" and NIR regions were the most influential variables (Figure 5a; Table 3). SWIR and VIS regions were also important but to a lesser degree (Figure 5a). For the classification of spectra by lineage at different sites, coefficients showed that similarly the "red edge" and NIR regions were the most influential variables. For classification of the normalized spectra by lineage only, coefficients for the two LD axes showed that the VIS, the "red-edge", and two regions in the SWIR were the most influential (Figure 5b; Table 3). The NIR region was no longer important for

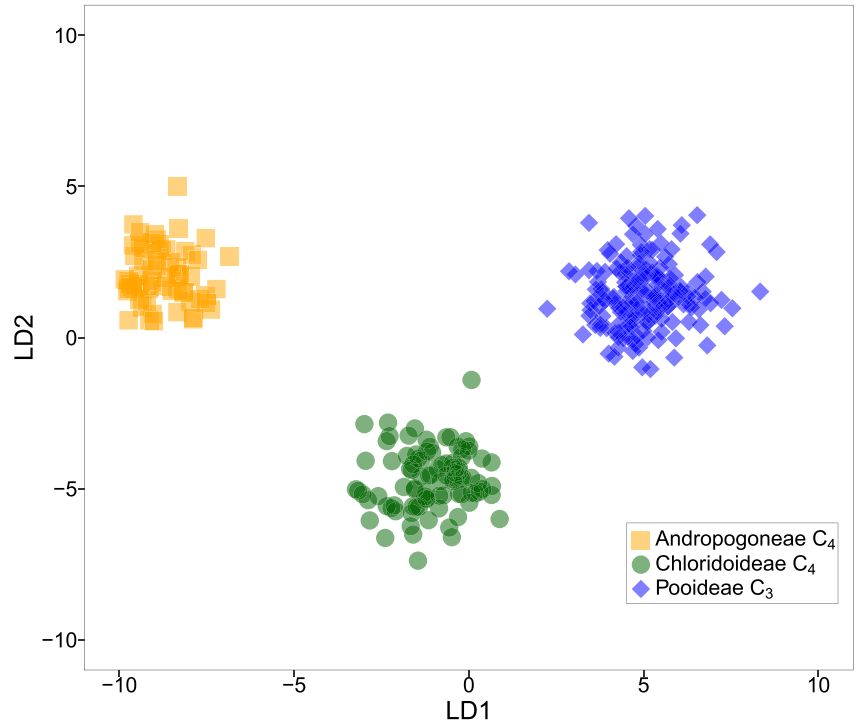

Figure 3. Linear Discriminant Analysis for classifying major grass evolutionary lineages based on the leaf reflectance spectra (400–2,400 nm). The first component (LD1) explains 80.8% of the variation in the spectra, whereas the second component (LD2) explains 19.2%.

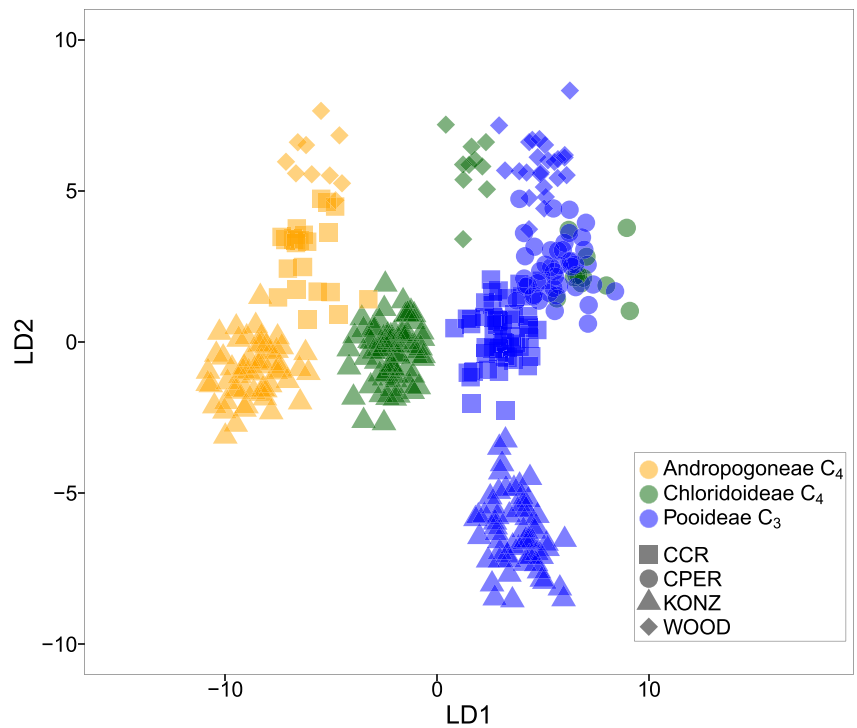

Figure 4. Linear Discriminant Analysis for each major lineage collected from different sites, which includes a different composition of species at each site (see Table 1). Eleven components were required to explain 100% of the variation in spectra, with the first two components explaining more than 57% of the variation in spectra.

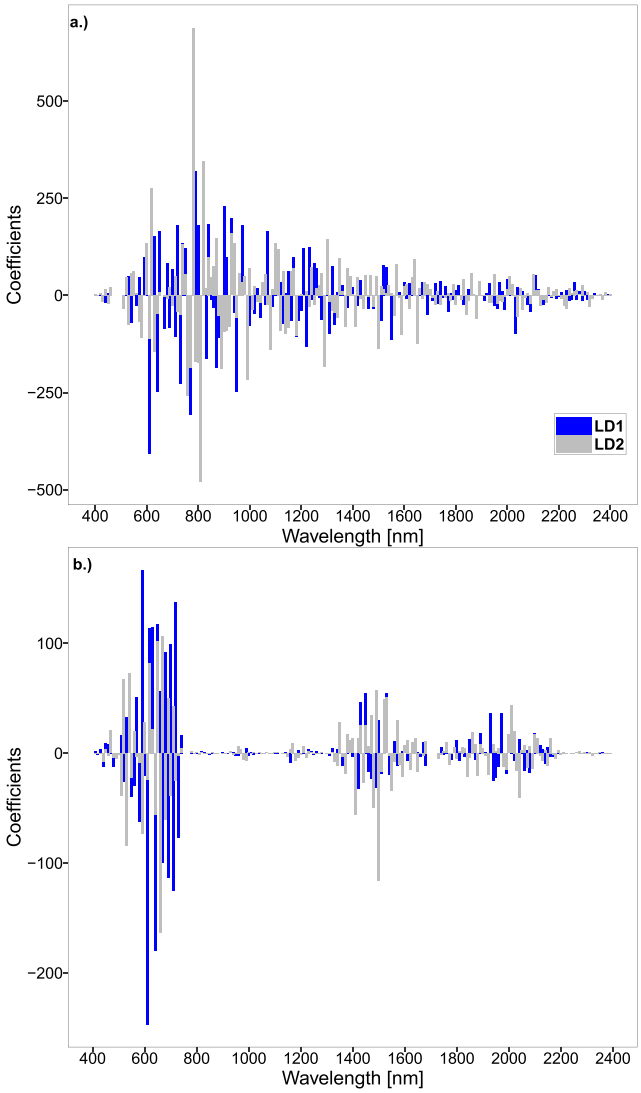

Figure 5. The Linear Discriminant Analysis (LDA) Coefficients are used to determine which spectral regions are influential in separating the dominant grass lineages. LDA coefficients using raw spectra for classifying dominant grass lineages (a). Coefficients of linear discriminants from the LDA model using the normalized spectra through continuum removal for classified dominant grass lineages (b).

classification when spectra were normalized, which is expected because the NIR is the highest reflectance region. The same regions were also important for classification of spectra by lineage at different sites.

3.3. Classification of Lineages Using Multispectral Data

When aggregating the leaf-level spectra to the bands available with Sentinel 2 and Landsat 8 OLI, the spectral resolution dropped over fifteenfold. Using the aggregated leaf-level spectra with Sentinel 2 bands, overall prediction accuracy was 85.2% and the Kappa coefficient was 0.76 (Table 4a). The first discriminant (LD1) explained 86.4% of the variance in the raw spectra and the second discriminant (LD2) explained 13.6% of the remaining variance (Figure 6a). Aggregating the leaf-level spectra to Landsat 8 OLI resulted in an overall prediction accuracy of 61.3% and the Kappa coefficient was 0.37 (Table 4b). The first discriminant (LD1) explained 67.8% of the variance in the raw spectra, the second discriminant (LD2) explained 32.2% of the remaining variance (Figure 6b).

4. Discussion

Grasslands and savannas cover substantial extents of the Earth's surface, amounting to over one-quarter of the terrestrial surface (Asner et al., 2004). We demonstrate an ability to differentiate ecologically dominant evolutionary lineages of North American grass species using solely leaf reflectance spectra. Our analysis is robust to site differences at peak greenness across the North American Great Plains. Within each lineage, species turnover at or among sites does not degrade these spectral features in the context of our study. Recent work using hyperspectral monitoring of grasslands has examined key biodiversity metrics such as alpha or beta taxonomic diversity and functional trait variation (Gholizadeh et al., 2019, 2022; Wang et al., 2022). In examining phylogenetic diversity, our results suggest that the ecological behavior of grasses can be accurately captured by "lineage functional types", which explicitly include evolutionary history as a framework for functional groupings (Griffith et al., 2020). These groupings reflect deep evolutionary branches within the grass phylogeny that relate to important trait differences.

Our analysis was robust to using either raw or normalized spectra, indicating that our classifiers were related to spectral features present regardless of overall leaf albedo (i.e., differences in leaf area or surface traits). However, different regions of the spectra were important for classification when examining absolute leaf reflectance (i.e., percent reflectance) or leaf reflectance that were normalized (i.e., differences in the shape of the reflectance curve). When using raw spectra, the most important regions for classification were the "red edge" (700–800 nm) and the NIR region (810–1300 nm). The "red edge" region is where infrared reflectance increases rapidly from the chlorophyll absorption region in the visible spectrum to the NIR region of high leaf reflectance. The red edge has been identified as important for separating C_3 and C_4 grass types because of its relationship to leaf nitrogen concentration (Shoko & Mutanga, 2017), though this region is more commonly thought to capture differences in chlorophyll absorption (Curran et al., 1990).

While we did not analyze leaf traits, in a recent analysis of grass leaf traits, the photosynthetic traits Vc_{max} (maximum carboxylation rate) and C:N was found to differ significantly among grass lineages, illustrating linkages between leaf N/chlorophyll content and overall photosynthetic activity (Donnelly et al., 2023). The NIR region is highly sensitive to leaf structural traits. Leaf structural traits such as specific leaf area and leaf dry matter content, as well as and leaf thickness for perennial species, are significantly different among grass lineages (Donnelly et al., 2023) and may have contributed to spectral separation. In addition, leaf surface traits such as pubescence or waxiness, can strongly affect NIR reflectance.

Table 3
Selected Features for the Raw and Normalized Spectra That Were Important for Classifying Dominant Grass Lineages and Dominant Grass Lineages at Different Sites

Spectral regions (nm)				
LDA model	VIS	Red edge	NIR	SWIR
Dominant Lineages (raw)	580–650	710–800	810–840, 870–910, 930–950, 970, 990, 1,070, 1,080, 1,100, 1,110, 1,140, 1,170, 1,180, 1,210–1,230, 1,290	1,300, 1,310, 1,350, 1,500, 1,550, 1,590, 1,640, 1,650, 2,030
Dominant Lineages (normalized)	510–550, 570–590, 610–690	700–730		1,410, 1,430, 1,450, 1,480–1,500, 1,520, 1,530, 1,930, 1,970, 2,010, 2,040
Dominant Lineages × Site (raw)	640	740–800	840, 870–910, 950, 960, 990, 1,000, 1,110, 1,120, 1,180, 1,190, 1,230, 1,260, 1,280	1,580
Dominant Lineages × Site (normalized)	540–560, 580, 590, 610, 620, 640–690	700–730		1,400–1,440, 1,460–1,480, 1,530, 1,540

In our data NIR reflectance was large (Figure 2) and can overwhelm important variation in other regions of the spectra. When spectra were normalized to remove differences in leaf albedo, the near infrared region of leaf spectra was less important for classification. Instead, in addition to the red-edge still being important, the visible region (530–690 nm) and two regions in the SWIR (1,410 nm–1,500 nm and 1,930 nm–1,970 nm) were the most important. Visible regions are known to be highly sensitive to chlorophyll *a* and *b* concentration (Gitelson & Merzlyak, 1998) suggesting an important difference in photosynthetic capacity among grass lineages. The SWIR region is sometimes related to leaf nitrogen content (Adjorlolo et al., 2012). More often, portions of the SWIR are linked to water content and the curing rate of leaves (Ceccato et al., 2001; Hunt & Yilmaz, 2007). Reflectance in the SWIR and visible region can be related because chlorophyll content and curing rate can covary (Ceccato

Table 4
Classification Matrices From LDA Models for Identifying Lineages Aggregated to Sentinel 2 (a) and Landsat 8 (b)

a.)

	Reference				
Prediction	Andropogoneae	Chloridoideae	Pooideae	Total	Prediction accuracy (%)
Andropogoneae	20	0	1	21	95.20%
Chloridoideae	3	15	5	23	65%
Pooideae	0	4	40	44	91%
Total	23	19	46	88	
Reference accuracy (%)	87%	80%	87%		
Overall classification accuracy = 85% and the Kappa statistic = 0.76					

b.)

	Reference				
Prediction	Andropogoneae	Chloridoideae	Pooideae	Total	Prediction accuracy (%)
Andropogoneae	13	0	8	21	61.90%
Chloridoideae	7	9	7	23	39%
Pooideae	4	8	32	44	73%
Total	24	17	47	88	
Reference accuracy (%)	54.17%	52.94%	68.09%		
Overall classification accuracy = 61% and the Kappa statistic = 0.37					

Note. Correctly identified lineages are shown on the diagonal while false positives and false negatives are shown on the off diagonals.

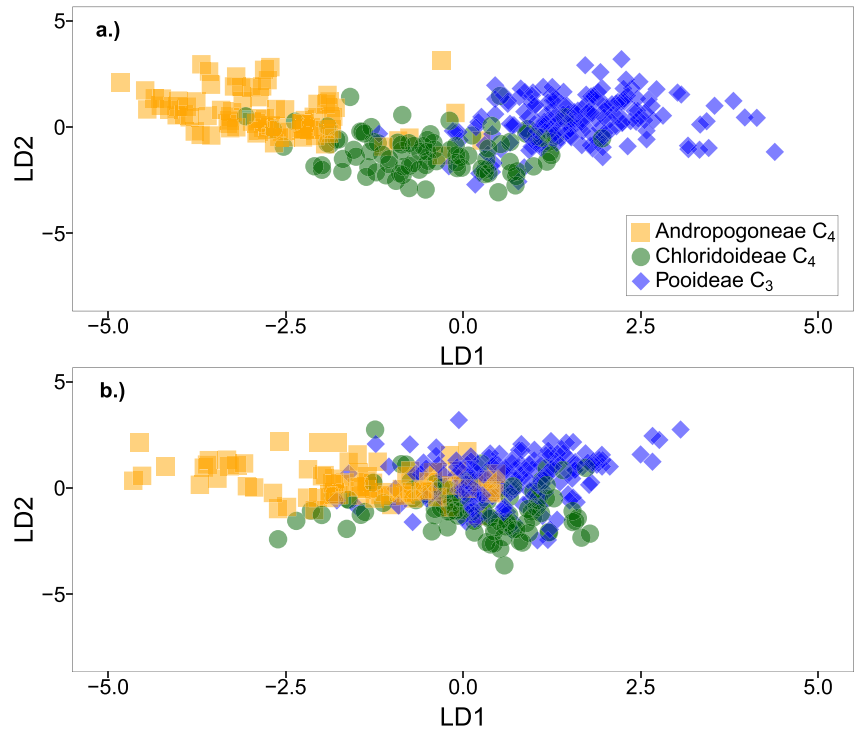

Figure 6. Linear Discriminant Analysis (LDA) for classifying major grass evolutionary lineages based on the leaf reflectance spectra using spectral bands that correspond to the spaceborne sensor Sentinel 2 (a) resulted in the first component (LD1) explaining 86.4% of the variation in the spectra and the second component (LD2) explaining 13.6%. Classifying grass lineages using spectral bands from the spaceborne sensor Landsat 8 (b) resulted in the first component (LD1) explaining 67.8% of the variation in the spectra while LD2 explains 32.2%.

et al., 2001). Curing rate can be an especially important trait for grasses, such as in the Andropogoneae lineage, that occur in regions with frequent fire.

Understanding variation in spectra, which provide an integrated measure of leaf traits that often covary (Cavender-Bares et al., 2017; Kothari & Schweiger, 2022), across different sites could provide insight into how plants function under changing environments. Furthermore, this understanding is needed for more accurate mapping using spectral endmembers. Although we classified lineages with high accuracy (>90%), some of the variability in leaf spectra was associated with site differences. This suggests that in addition to lineage identity, site differences may have contributed to our spectral separation. This result is in part related to species turnover at each site but also apparent in the spectra of the same species at different sites (Figure S2 and S3). Plant spectra of the same species can vary in different environmental contexts (Andrew & Ustin, 2008) given that different genotypes and intraspecific traits are known to respond to changing climate conditions, resource limitations, and biotic interactions, in addition to life history and ontogeny (although in our case spectra were collected during peak greenness at each site; Figure S3). The competitive environment and presence of co-occurring species has rarely been considered in spectral endmember mapping but could affect available resources and thus plant traits (Andrew & Ustin, 2008). For example, imaging spectroscopy detected decreased foliar nitrogen concentrations of a native tree species in Hawaii in the presence of a nutrient-demanding invasive plant (Asner & Vitousek, 2005). Because plasticity can be an adaptive trait (Bachle & Nippert, 2018; Bradshaw, 1965; Donoghue & Edwards, 2014), examining which lineages show more or less variability in their spectra across environmental gradients, and in which spectral regions, will help us understand grassland responses to future environmental change.

We did not identify explicit relationships between leaf spectra and traits, which limits mechanistic understanding of leaf traits that underpin differences in leaf spectral reflectance. Furthermore, spectra-trait relationships can potentially be used to develop trait maps across larger regions and forecast how altered future climates may drive changes in ecosystem functions. In addition, our four sites did not provide coverage of hotter and drier regions of

the Great Plains where the Chloridoideae lineage is dominant and resource constraints may be different than in other regions. Of the three dominant lineages we examined, Chloridoideae had the lowest classification accuracy (Table 2). Chloridoideae spectra did not appear to be more variable compared to other lineages (Figure 1) but did appear to overlap with other lineages (Figure 4), perhaps because we did not accurately capture Chloridoideae dominant regions. We note that leaf spectra may differ for different species due to internal or external traits and the effect of these individual traits on leaf spectra is often much smaller than the effect of site. Therefore, how transferable our results are across diverse grasslands of North America or globally is not clear. Additionally, in natural settings, plant canopies can interact with light differently than a single leaf, thus canopy structural parameters such as leaf area index and leaf angle distribution are required for a full upscaling to satellite observations. The high species diversity at fine spatial scales in many grassland communities is also a challenging consideration in future attempts to upscale leaf-level spectra across landscapes, though mapping lineage composition may be more tractable. Future work using remote sensing imagery should identify the strength of relationships between leaf spectra and canopy spectra with varying compositions of structural and taxonomic diversity and expand the environmental coverage of sites to fully explore variation among grass lineages and sites.

Our work shows that detailed spectral signatures at the leaf-level can diagnose dominant grass lineages, providing insight into the origins of biodiversity patterns and potential differences in ecological function in one of the Earth's largest biomes. It is unclear if classification accuracy into lineages using leaf spectra has a similar accuracy when using plot or canopy scale spectra. However expanding this work to map the distributions of these lineages across landscapes would provide a major improvement over studies focused on C_3–C_4 grass distributions; these studies have previously provided an incomplete picture of grassland functional diversity in ecological modeling and macrosystem ecology (Griffith et al., 2020; Still et al., 2019). Existing multispectral satellite sensors, such as those on Landsat and Sentinel, provide longer records and more frequent observations than available on proposed hyperspectral missions, and therefore can be complementary to hyperspectral data. We found, however, that the poorer spectral resolution and spectral coverage are not optimal for detecting differences among the most dominant grass lineages at the leaf level (Tables 4a and 4b). Information is lost when using spectral regions available on multispectral sensors compared to the full hyperspectral range. Sentinel 2, which includes a band covering the red-edge, resulted in much higher classification accuracy than Landsat 8, which does not include any bands in the red-edge. This study identifies added information that repeated and global hyperspectral imagery might bring to macroecological understanding compared to multispectral remote sensing (e.g., Cawse-Nicholson et al., 2022, 2023).

Our work reveals exciting potential for broad mapping of dominant grass evolutionary lineages across diverse grassy landscapes. Advances in grassland macroecology require accurately mapping the spatial distribution and environmental context of functionally distinct grass lineages. While decades of multispectral satellite observations have revealed the potential for systematic observations of plant species distributions and biodiversity patterns across the globe (e.g., Skidmore et al., 2021), important spectral regions for separating grass lineages are not well covered in existing multispectral sensors. Our work illustrates the need for future hyperspectral satellite missions to advance macroecological understanding.

Data Availability Statement

All data used for the creation of this manuscript are available at Zenodo DOI 10.5281/zenodo.10575929. Figures were made with "ggplot2" version 3.3.6 (Wickham, 2016). Maps were created using "tmap" version 3.3-3 (Tennekes, 2018). Part of the software used with this manuscript for the calculation and jump correction is licensed under MIT and published on GitHub https://github.com/EnSpec/SpecDAL.

Acknowledgments
This work was supported by the National Science Foundation (NSF) and the National Ecological Observatory Network Program (NEON). NEON is a program sponsored by the NSF and operated under cooperative agreement by Battelle Memorial Institute. We thank the site managers at Konza Prairie, Colorado Plains Experimental Range, Chase Lake National Wildlife Refuge, and Cedar Creek Ecosystem Reserve for assistance and access to sites. SP, RS, RCD, JBN, BRH, CJS, and DMG were supported by National Science Foundation awards 1926108, 1926431, 1926114, 1926345, and 1440484. WJR acknowledges support by the Office of Biological and Environmental Research of the U.S. Department of Energy Office of Science in the Regional and Global Model Analysis program for the RUBISCO Scientific Focus Area. Lawrence Berkeley National Laboratory (LBNL) is managed by the University of California for the U.S. Department of Energy under contract DE-AC02-05CH11231.

References

Adjorlolo, C., Mutanga, O., Ismail, R., & Cho, M. A. (2012). Optimizing spectral resolutions for the classification of C_3 and C_4 grass species, using wavelengths of known absorption features. *Journal of Applied Remote Sensing*, *6*(1), 063560–063561. https://doi.org/10.1117/1.JRS.6.063560

Aliscioni, S., Bell, H. L., Besnard, G., Christin, P. A., Columbus, J. T., Duvall, M. R., et al. (2012). New grass phylogeny resolves deep evolutionary relationships and discovers C4 origins. *New Phytologist*, *193*(2), 304–312. https://doi.org/10.1111/j.1469-8137.2011.03972.x

Andrew, M. E., & Ustin, S. L. (2008). The role of environmental context in mapping invasive plants with hyperspectral image data. *Remote Sensing of Environment*, *112*(12), 4301–4317. https://doi.org/10.1016/J.RSE.2008.07.016

Asner, G. P., Elmore, A. J., Olander, L. P., Martin, R. E., & Harris, A. T. (2004). Grazing systems, ecosystem responses, and global change. *Annual Review of Environment and Resources*, *29*(1), 261–299. https://doi.org/10.1146/annurev.energy.29.062403.102142

Asner, G. P., & Martin, R. E. (2011). Canopy phylogenetic, chemical and spectral assembly in a lowland Amazonian forest. *New Phytologist*, *189*(4), 999–1012. https://doi.org/10.1111/j.1469-8137.2010.03549.x

Asner, G. P., & Vitousek, P. M. (2005). Remote analysis of biological invasion and biogeochemical change. *Proceedings of the National Academy of Sciences of the United States of America*, *102*(12), 4383–4386. https://doi.org/10.1073/PNAS.0500823102/SUPPL_FILE/00823FIG7.JPG

Bachle, S., & Nippert, J. B. (2018). Physiological and anatomical trait variability of dominant C_4 grasses. *Acta Oecologica*, *93*, 14–20. https://doi.org/10.1016/j.actao.2018.10.007

Bachle, S., & Nippert, J. B. (2022). Physiological ecology-original research Climate variability supersedes grazing to determine the anatomy and physiology of a dominant grassland species. *Oecologia*, *198*(2), 345–355. https://doi.org/10.1007/s00442-022-05106-x

Bachmann, M., & Heldens, W. (2006). AS Toolbox and Processing of field spectra User's manual. Retrieved from http://www.ares.caf.dlr.de

Bond, W. J., & Midgley, G. F. (2000). A proposed CO_2-controlled mechsanism of woody plant invasion in grasslands and savannas. *Global Change Biology*, *6*(8), 865–869. https://doi.org/10.1046/J.1365-2486.2000.00365.X

Bond, W. J., Woodward, F. I., & Midgley, G. F. (2005). The global distribution of ecosystems in a world without fire. *New Phytologist*, *165*(2), 525–538. https://doi.org/10.1111/J.1469-8137.2004.01252.X

Bradshaw, A. D. (1965). Evolutionary significance of phenotypic plasticity in plants. *Advances in Genetics*, *13*(C), 115–155. https://doi.org/10.1016/S0065-2660(08)60048-6

Carroll, O., Batzer, E., Bharath, S., Borer, E. T., Campana, S., Esch, E., et al. (2022). Nutrient identity modifies the destabilising effects of eutrophication in grasslands. *Ecology Letters*, *25*(4), 754–765. https://doi.org/10.1111/ELE.13946

Cavender-Bares, J., Gamon, J. A., Hobbie, S. E., Madritch, M. D., Meireles, J. E., Schweiger, A. K., & Townsend, P. A. (2017). Harnessing plant spectra to integrate the biodiversity sciences across biological and spatial scales. *American Journal of Botany*, *104*(7), 966–969. https://doi.org/10.3732/AJB.1700061

Cavender-Bares, J., Meireles, J. E., Couture, J. J., Kaproth, M. A., Kingdon, C. C., Singh, A., et al. (2016). Associations of leaf spectra with genetic and phylogenetic variation in oaks: Prospects for remote detection of biodiversity. *Remote Sensing*, *8*(3), 221. https://doi.org/10.3390/RS8030221

Cavender-Bares, J., Schneider, F. D., Santos, M. J., Armstrong, A., Carnaval, A., Dahlin, K. M., et al. (2022). Integrating remote sensing with ecology and evolution to advance biodiversity conservation. *Nature Ecology & Evolution*, *6*(5), 506–519. https://doi.org/10.1038/S41559-022-01702-5

Cawse-Nicholson, K., Raiho, A. M., Thompson, D. R., Hulley, G. C., Miller, C. E., Miner, K. R., et al. (2023). Surface biology and geology imaging spectrometer: A case study to optimize the mission design using intrinsic dimensionality. *Remote Sensing of Environment*, *290*, 113534. https://doi.org/10.1016/j.rse.2023.113534

Cawse-Nicholson, K., Raiho, A. M., Thompson, D. R., Hulley, G. C., Miller, C. E., Miner, K. R., et al. (2022). Intrinsic dimensionality as a metric for the impact of mission design parameters. *Journal of Geophysical Research: Biogeosciences*, *127*(8), e2022JG006876. https://doi.org/10.1029/2022jg006876

Cawse-Nicholson, K., Townsend, P. A., Schimel, D., Assiri, A. M., Blake, P. L., Buongiorno, M. F., et al. (2021). NASA's surface biology and geology designated observable: A perspective on surface imaging algorithms. *Remote Sensing of Environment*, *257*, 112349. https://doi.org/10.1016/J.RSE.2021.112349

Ceccato, P., Flasse, S., Tarantola, S., Jacquemoud, S., & Grégoire, J. M. (2001). Detecting vegetation leaf water content using reflectance in the optical domain. *Remote Sensing of Environment*, *77*(1), 22–33. https://doi.org/10.1016/S0034-4257(01)00191-2

Clark, R. N., & Roush, T. L. (1984). Reflectance spectroscopy: Quantitative analysis techniques for remote sensing applications. *Journal of Geophysical Research*, *89*(B7), 6329–6340. https://doi.org/10.1029/jb089ib07p06329

Crisp, M. D., Arroyo, M. T. K., Cook, L. G., Gandolfo, M. A., Jordan, G. J., McGlone, M. S., et al. (2009). Phylogenetic biome conservatism on a global scale. *Nature*, *458*(7239), 754–756. https://doi.org/10.1038/NATURE07764

Curran, P. J., Dungan, J. L., & Gholz, H. L. (1990). Exploring the relationship between reflectance red edge and chlorophyll content in slash pine. *Tree Physiology*, *7*(1–2-3–4), 33–48. https://doi.org/10.1093/TREEPHYS/7.1-2-3-4.33

Donnelly, R. C., Wedel, E. R., Taylor, J. H., Nippert, J. N., Helliker, B. R., Riley, W. J., et al. (2023). Evolutionary lineage explains trait variation among 75 coexisting grass species. *New Phytologist*, *239*(3), 875–887. https://doi.org/10.1111/nph.18983

Donoghue, M. J., & Edwards, E. J. (2014). Biome shifts and niche evolution in plants. *Annual Review of Ecology Evolution and Systematics*, *45*(1), 547–572. https://doi.org/10.1146/ANNUREV-ECOLSYS-120213-091905

Edwards, E. J., & Smith, S. A. (2010). Phylogenetic analyses reveal the shady history of C_4 grasses. *Proceedings of the National Academy of Sciences of the United States of America*, *107*(6), 2532–2537. https://doi.org/10.1073/PNAS.0909672107/SUPPL_FILE/PNAS.200909672SI.PDF

Edwards, E. J., & Still, C. J. (2008). Climate, phylogeny and the ecological distribution of C_4 grasses. *Ecology Letters*, *11*(3), 266–276. https://doi.org/10.1111/J.1461-0248.2007.01144.X

Garcia-Allende, P. B., Conde, O. M., Mirapeix, J., Cobo, A., & Lopez-Higuera, J. M. (2008). Quality control of industrial processes by combining a hyperspectral sensor and Fisher's linear discriminant analysis. *Sensors and Actuators B: Chemical*, *129*(2), 977–984. https://doi.org/10.1016/j.snb.2007.09.036

Gholizadeh, H., Friedman, M. S., McMillan, N. A., Hammond, W. M., Hassani, K., Sams, A. V., et al. (2022). Mapping invasive alien species in grassland ecosystems using airborne imaging spectroscopy and remotely observable vegetation functional traits. *Remote Sensing of Environment*, *271*, 112887. https://doi.org/10.1016/J.RSE.2022.112887

Gholizadeh, H., Gamon, J. A., Townsend, P. A., Zygielbaum, A. I., Helzer, C. J., Hmimina, G. Y., et al. (2019). Detecting prairie biodiversity with airborne remote sensing. *Remote Sensing of Environment*, *221*, 38–49. https://doi.org/10.1016/j.rse.2018.10.037

Gitelson, A. A., & Merzlyak, M. N. (1998). Remote sensing of chlorophyll concentration in higher plant leaves. *Advances in Space Research*, *22*(5), 689–692. https://doi.org/10.1016/S0273-1177(97)01133-2

Griffith, D. M., Byrd, K. B., Anderegg, L. D. L., Allan, E., Gatziolis, D., Roberts, D., et al. (2023a). Capturing patterns of evolutionary relatedness with reflectance spectra to model and monitor biodiversity. *Proceedings of the National Academy of Sciences*, *120*(24), e2215533120. https://doi.org/10.1073/pnas.2215533120

Griffith, D. M., Byrd, K. B., Taylor, N., Allan, E., Bittner, L., O'Brien, B., et al. (2023b). Variation in leaf reflectance spectra across the California flora partitioned by evolutionary history, geographic origin, and deep time. *Journal of Geophysical Research: Biogeosciences*, *128*(2), e2022JG007160. https://doi.org/10.1029/2022jg007160

Griffith, D. M., Lehmann, C. E., Strömberg, C. A., Parr, C. L., Pennington, R. T., Sankaran, M., et al. (2017). Comment on "The extent of forest in dryland biomes". *Science*, *358*(6365), eaao1309. https://doi.org/10.1126/science.aao0166

Griffith, D. M., Osborne, C. P., Edwards, E. J., Bachle, S., Beerling, D. J., Bond, W. J., et al. (2020). Lineage-based functional types: Characterising functional diversity to enhance the representation of ecological behaviour in land surface models. *New Phytologist*, *228*(1), 15–23. https://doi.org/10.1111/NPH.16773

Hellmann, C., Große-Stoltenberg, A., Lauströer, V., Oldeland, J., & Werner, C. (2015). Retrieving nitrogen isotopic signatures from fresh leaf reflectance spectra: Disentangling δ15N from biochemical and structural leaf properties. *Frontiers in Plant Science*, *6*(MAY). https://doi.org/10.3389/FPLS.2015.00307/ABSTRACT

Hunt, Jr., E. R., & Yilmaz, M. T. (2007). *Remote sensing of vegetation water content using shortwave infrared reflectances*. In *Remote Sensing and Modeling of Ecosystems for Sustainability IV*, Vol. 6679, 15–22. SPIE. https://doi.org/10.1117/12.734730

Jensen, J. R. (2007). *Remote sensing of the environment: An Earth resource perspective* (2nd ed.). Pearson Prentice Hall.

Kothari, S., & Schweiger, A. K. (2022). Plant spectra as integrative measures of plant phenotypes. *Journal of Ecology*, *110*(11), 2536–2554. https://doi.org/10.1111/1365-2745.13972

Kuhn, M. (2008). Building predictive models in R using the caret package. *Journal of Statistical Software*, *28*, 1–26. https://doi.org/10.18637/jss.v028.i05

Lehmann, C. E., Griffith, D. M., Simpson, K. J., Anderson, T. M., Archibald, S., Beerling, D. J., et al. (2019). Functional diversification enabled grassy biomes to fill global climate space. BioRxiv.583625.

Lehnert, L. W., Meyer, H., Obermeier, W. A., Silva, B., Regeling, B., Thies, B., & Bendix, J. (2019). Hyperspectral data analysis in R: The hsdar package. *Journal of Statistical Software*, *89*(12), 1–23. https://doi.org/10.18637/JSS.V089.I12

Liu, H., Edwards, E. J., Freckleton, R. P., & Osborne, C. P. (2012). Phylogenetic niche conservatism in C_4 grasses. *Oecologia*, *170*(3), 835–845. https://doi.org/10.1007/S00442-012-2337-5

Meireles, J. E., Cavender-Bares, J., Townsend, P. A., Ustin, S., Gamon, J. A., Schweiger, A. K., et al. (2020). Leaf reflectance spectra capture the evolutionary history of seed plants. *New Phytologist*, *228*(2), 485–493. https://doi.org/10.1111/NPH.16771

Mutanga, O., & Skidmore, A. K. (2004). Integrating imaging spectroscopy and neural networks to map grass quality in the Kruger National Park, South Africa. *Remote Sensing of Environment*, *90*(1), 104–115. https://doi.org/10.1016/j.rse.2003.12.004

R Core Team. (2022). No Title. [Software] Retrieved from https://www.r-project.org/

Rocchini, D., Santos, M. J., Ustin, S. L., Féret, J. B., Asner, G. P., Beierkuhnlein, C., et al. (2022). The spectral species concept in living color. *Journal of Geophysical Research: Biogeosciences*, *127*(9), e2022JG007026. https://doi.org/10.1029/2022JG007026

Schweiger, A. K., Cavender-Bares, J., Townsend, P. A., Hobbie, S. E., Madritch, M. D., Wang, R., et al. (2018). Plant spectral diversity integrates functional and phylogenetic components of biodiversity and predicts ecosystem function. *Nature Ecology & Evolution*, *2*(6), 976–982. https://doi.org/10.1038/s41559-018-0551-1

Seetohul, L. N., Scott, S. M., O'Hare, W. T., Ali, Z., & Islam, M. (2013). Discrimination of Sri Lankan black teas using fluorescence spectroscopy and linear discriminant analysis. *Journal of the Science of Food and Agriculture*, *93*(9), 2308–2314. https://doi.org/10.1002/jsfa.6044

Serbin, S. P., Singh, A., McNeil, B. E., Kingdon, C. C., & Townsend, P. A. (2014). Spectroscopic determination of leaf morphological and biochemical traits for northern temperate and boreal tree species. *Ecological Applications*, *24*(7), 1651–1669. https://doi.org/10.1890/13-2110.1

Shoko, C., & Mutanga, O. (2017). Seasonal discrimination of C_3 and C_4 grasses functional types: An evaluation of the prospects of varying spectral configurations of new generation sensors. *International Journal of Applied Earth Observation and Geoinformation*, *62*, 47–55. https://doi.org/10.1016/J.JAG.2017.05.015

Skidmore, A. K., Coops, N. C., Neinavaz, E., Ali, A., Schaepman, M. E., Paganini, M., et al. (2021). Priority list of biodiversity metrics to observe from space. *Nature Ecology & Evolution*, *5*(7), 896–906. https://doi.org/10.1038/s41559-021-01451-x

Soreng, R. J., Peterson, P. M., Romaschenko, K., Davidse, G., Teisher, J. K., Clark, L. G., et al. (2017). A worldwide phylogenetic classification of the Poaceae (Gramineae) II: An update and a comparison of two 2015 classifications. *Journal of Systematics and Evolution*, *55*(4), 259–290. https://doi.org/10.1111/JSE.12262/SUPPINFO

Still, C. J., Berry, J. A., Ribas-Carbo, M., & Helliker, B. R. (2003). The contribution of C_3 and C_4 plants to the carbon cycle of a tallgrass prairie: An isotopic approach. *Oecologia*, *136*, 347–359. https://doi.org/10.1007/s00442-003-1274-8

Still, C. J., Cotton, J. M., & Griffith, D. M. (2019). Assessing earth system model predictions of C_4 grass cover in North America: From the glacial era to the end of this century. *Global Ecology and Biogeography*, *28*(2), 145–157. https://doi.org/10.1111/GEB.12830

Strömberg, C. A. E., & Staver, A. C. (2022). The history and challenge of grassy biomes. *Science*, *377*(6606), 592–593. https://doi.org/10.1126/SCIENCE.ADD1347

Taylor, S. H., Hulme, S. P., Rees, M., Ripley, B. S., Woodward, F. I., & Osborne, C. P. (2010). Ecophysiological traits in C_3 and C_4 grasses: A phylogenetically controlled screening experiment. *New Phytologist*, *185*, 780–791. https://doi.org/10.1111/j.1469-8137.2009.03102.x

Tennekes, M. (2018). tmap: Thematic maps in R [Software]. Journal of Statistical Software, *84*(6), 1–39. https://doi.org/10.18637/jss.v084.i06

Ustin, S. L., Roberts, D. A., Gamon, J. A., Asner, G. P., & Green, R. O. (2004). Using imaging spectroscopy to study ecosystem processes and properties. *BioScience*, *54*(6), 523. https://doi.org/10.1641/0006-3568(2004)054[0523:uistse]2.0.co;2

Wang, D., Qiu, P., Wan, B., Cao, Z., & Zhang, Q. (2022). Mapping α- and β-diversity of mangrove forests with multispectral and hyperspectral images. *Remote Sensing of Environment*, *275*, 113021. https://doi.org/10.1016/J.RSE.2022.113021

Wickham, H. (2016). ggplot2: Elegant graphics for data analysis. Springer-Verlag New York. [Software] https://ggplot2.tidyverse.org